

Electron states of a wide quantum well in a tilted magnetic field

M. Shayegan, T. Sajoto, J. Jo, and M. Santos

Department of Electrical Engineering, Princeton University, Princeton, New Jersey 08544

H. D. Drew

Department of Physics and Astronomy, University of Maryland, College Park, Maryland 20742

(Received 12 May 1989)

The magnetoresistance of an electron system in a selectively doped, wide quantum well of $\text{Al}_x\text{Ga}_{1-x}\text{As}$ is studied with the magnetic field (\mathbf{B}) tilted slightly away from the sample plane. We observe a dramatic manifestation of the subband-Landau-level coupling. At low B , we observe magnetoresistance oscillations which are not periodic in $1/B$, and are related to the magnetic depopulation of the hybrid (electric-magnetic) subbands. At higher fields, Shubnikov-de Haas-like oscillations (periodic in $1/B$) are observed as the Fermi level crosses the quantized energy levels associated with the lowest hybrid subband.

The energy-level structure of an electron system spatially confined in a narrow quantum well is principally controlled by the well width. For a moderately strong magnetic field B applied in a direction tilted with respect to the plane of the electron system (the x - y plane), the spatial quantization still dominates the form of the wave function. This is true as long as $l \gg w$, where $l = (\hbar/eB)^{1/2}$ is the magnetic length and w is the well width. The motion in the x - y plane is quantized into Landau levels with the cyclotron frequency determined by the component of B normal to the plane.¹ In a sufficiently strong B (so that $l \ll w$), however, the electron orbits are constrained to spiral along the oblique magnetic field lines. In this Rapid Communication, we report the observation of such electron states, which we call *oblique* states, in a wide quantum-well system.

The structure consists of a selectively doped, wide, parabolically graded well which, owing to the self-consistent Poisson potential, approximates a wide square well of width $w \approx 1000 \text{ \AA}$.²⁻⁴ Magnetotransport measurements, at low temperatures and for magnetic fields oriented close to the sample plane, reveal two kinds of characteristic behavior. At low field ($B \leq 2 \text{ T}$), magnetic depopulation of hybrid (electric and magnetic) subbands, manifested by strong oscillations in the magnetoresistance, occurs. In the range of $B \geq 2 \text{ T}$, we observe Shubnikov-de Haas-like oscillations which are periodic in $1/B$ and can be associated with the crossing of the Fermi energy with the oblique states. These observations provide clear evidence for the oblique states in a strong tilted magnetic field.

The details of our structure and its growth parameters were given previously.^{2,3} It consists of a wide, undoped, parabolic $\text{Al}_x\text{Ga}_{1-x}\text{As}$ well bounded by undoped (spacer) and doped layers of $\text{Al}_y\text{Ga}_{1-y}\text{As}$ ($y > x$) on two sides. Classically, once the electrons are transferred into this well, they screen the parabolic potential and a system of almost uniformly distributed electrons in a flat potential can be expected.²⁻⁷ In order to determine the quantum-mechanical subband structure of the electron system, we performed self-consistent calculations by solving Poisson and Schrödinger equations, and taking into account the

exchange-correlation via local-density-functional approximation.^{3,4} The calculation indicates that for the measured electron areal density in our structure ($n_s \approx 2.4 \times 10^{11} \text{ cm}^{-2}$), four electric subbands are occupied at $B=0$. It is interesting to note that despite the relatively small number of occupied subbands, the electron density is fairly constant over a wide distance ($\sim 1000 \text{ \AA}$).³⁻⁵ If the effective width of the wave function is taken to be $\approx 1000 \text{ \AA}$, then the three-dimensional electron density in the well is $\approx 2.4 \times 10^{16} \text{ cm}^{-3}$.

To measure the transport coefficients, contacts were made by alloying indium in a hydrogen atmosphere at 400°C for 3-5 min. The sample was mounted in a ^3He cryostat with a tilting stage which allowed the sample rotation so that \mathbf{B} could be tilted with respect to the sample (x - y) plane. The sample current was along the \hat{x} direction, and \mathbf{B} was applied in the x - z plane. We denote the angle between \mathbf{B} and the sample plane by θ .

The data are shown in Fig. 1. We first discuss the two cases $\theta=0^\circ$ and 90° . For $\theta=90^\circ$, we measure the conventional transverse (ρ_{xx}) and the Hall (ρ_{xy}) resistivities. The low-temperature ($T \approx 0.5 \text{ K}$) ρ_{xx} and ρ_{xy} data exhibit integral quantum Hall effect for $B \gtrsim 2 \text{ T}$. The vertical arrows in Fig. 1 indicate the Landau-level filling factors (ν) at which the integral quantum Hall effect is observed. The positions of ρ_{xx} minima in this field range are consistent with an electron areal density $n_s = 2.4 \times 10^{11} \text{ cm}^{-2}$. In the range of $B \lesssim 2 \text{ T}$, however, the oscillations in ρ_{xx} contain several frequencies. To determine these frequencies, which are directly proportional to the areas of the Fermi surface cross sections, we calculated the Fourier transform of the ρ_{xx} vs $1/B$ (in the range of $B < 0.75 \text{ T}$) (Ref. 4). We then determined the subband densities from the measured cross sections. The measured densities are in excellent agreement with the subband densities obtained from the self-consistent calculations,⁴ providing quantitative evidence for the realization of the electron system described above.

When $\theta=0^\circ$, the longitudinal resistivity (ρ_l) is measured.⁸ The low-field ρ_l data (Fig. 1) show oscillations which are *not* periodic in $1/B$. With the magnetic field applied parallel to the quantum well, the potential due to the

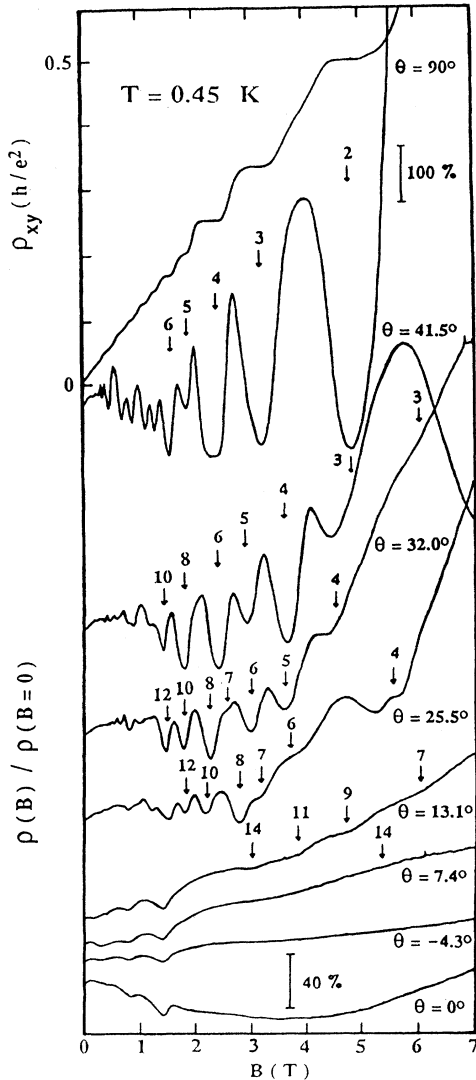


FIG. 1. The magnetotransport data measured at different orientations of the magnetic field (B) with respect to the sample plane are shown. The top two traces were measured at $\theta=90^\circ$, and correspond to the conventional ρ_{xy} and ρ_{xx} transport coefficients. The other traces were measured at the indicated θ . The scale for the ρ_{xy} (at $\theta=90^\circ$) is given on the left. The scale for the rest of the traces is given by the line marked 100%, except for the trace at $\theta=0^\circ$ whose scale is indicated by the line marked 40%.

magnetic field confinement as well as that due to the well must be considered. The result of such a mixed (electric and magnetic) potential is a nonlinear energy versus B fan diagram in which the energy levels at $B=0$ are determined by the well potential, while as $B \rightarrow \infty$, they approach the bulk Landau levels.⁹ This is schematically shown in Fig. 2. At $B=0$, the energy levels E_n for our self-consistent potential^{3,4} are shown. Also shown are the bulk Landau levels (indexed by N). The solid curves represent the energy versus B fan diagram. Determination of these curves for our potential via self-consistent calculations (in the presence of a magnetic field) must be done numerically. For the sake of illustration, we calculated

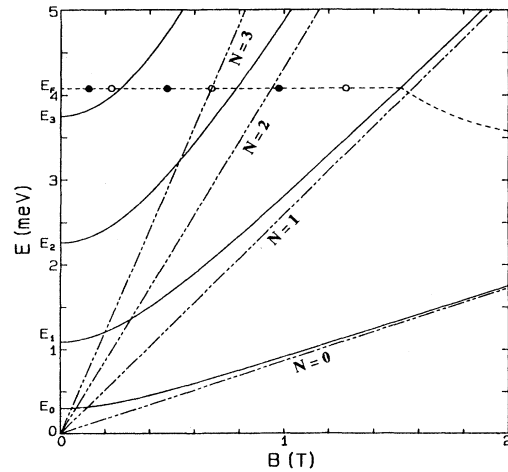


FIG. 2. Energy vs B fan diagram corresponding to the case $\theta=0^\circ$ is shown. At $B=0$ the energies for the electric subbands E_n are indicated. The dashed lines represent the bulk Landau levels (indexed by N). Note that as $B \rightarrow \infty$, $E_n(B) \rightarrow E_N(B)$. Spin splitting of the levels in the field range shown is small and is neglected here. The solid curves schematically show the hybrid (electric and magnetic) energy levels. The position of the Fermi level E_F is schematically shown by the dotted curve. Solid and open circles indicate the experimentally observed maxima in ρ_l and minima in $d\rho_l/dB$, respectively.

the energies

$$E_n(B) = \{[E_n(B=0)]^2 + (n + \frac{1}{2})^2 \hbar^2 \omega_c^2\}^{1/2}, \quad (1)$$

where $\omega_c = eB/m^*$ is the cyclotron frequency. In the case of a parabolic confining potential, Eq. (1) gives the exact $E_n(B)$.¹⁰ In Fig. 2 we have also indicated the position of E_F . At $B=0$, $E_F=4.08$ meV, and as B increases E_F is expected to behave as shown schematically by the dotted lines.¹¹ As the magnetic field is raised from zero, the degeneracy of the levels increases and magnetic depopulation of the levels occurs.^{9,12} Determination of the exact magnetic fields at which the subbands are depopulated from the line shape (positions of maxima and minima) of ρ_l is not straightforward.^{9,12-14} Intuitively, since the subband depopulation reduces the intersubband scattering, it is expected to result in a higher carrier mobility. An enhancement of the mobility, manifested by a negative magnetoresistance, was in fact observed by Englert *et al.*¹⁴ in a GaAs/Al_xGa_{1-x}As heterostructure and was attributed to the subband depopulation. More recently, Yoshino, Sakaki, and Hotta⁹ associated the maxima in ρ_l with the crossings of E_F with the energy levels, while Zrenner *et al.*¹³ have argued that the maxima in $d\sigma_l/dB$ (where $\sigma_l = \rho_l^{-1}$) correspond to these crossings. In Fig. 2, we have indicated our observed ρ_l maxima (solid circles) as well as the positions of the minimum slope in ρ_l following these maxima (open circles). The open circles seem to better correspond to the crossings of E_F with the energy levels. We emphasize, however, that Fig. 2 cannot be used for a detailed, quantitative comparison between the experimental data and the calculations. We only draw a main conclusion that the data provide strong evidence that four electric subbands are occupied at $B=0$, and that they be-

come depopulated in the low-field range ($B \lesssim 1.5$ T).

Figure 2 indicates that once E_F has crossed the $n=1$ level, there should be no more oscillations in ρ .¹⁵ With a finite angle between B and the plane of the sample, however, the motion parallel and perpendicular to the plane becomes coupled and the situation becomes more complicated. The Hamiltonian for the case of a magnetic field oriented at an angle θ with respect to the x axis in the x - z plane is given by

$$H = [p_y + eB(z \cos\theta - x \sin\theta)]^2/2m^* + p_z^2/2m^* + p_x^2/2m^* + V(z), \quad (2)$$

where $V(z)$ is the self-consistent confining potential. The general solutions to H are stationary states in the x - z plane and plane waves in the y direction. The spectrum is discrete with a degeneracy equal to $(eB/h)\sin\theta$. For the case of a quadratic potential $V(z)$, this problem can be solved analytically and describes coupled harmonic oscillator and Landau-level orbits.^{10,16} The low-lying states are then a set of equally spaced levels with a spacing of $\hbar\Omega\sin\theta$ where Ω is the frequency of the harmonic-oscillator states in zero magnetic field. For the sake of illustration, in Fig. 3 we show the energy spectrum calculated for a parabolic well whose zero-field subband energies are of the same order as those of our well (we used $\hbar\Omega = 1$ meV). The calculation is for $\theta = 10^\circ$. Also shown in Fig. 3 is the position of E_F as a function of B , using the fact that the degeneracy of each of the quantized energy levels is equal to $(2eB/h)\sin\theta$.^{10,16} In principle, if the magnetoresistance is measured at finite θ , it should show oscillations as E_F crosses each of the energy levels. In a real system, however, the energy levels will have finite widths (because of disorder). Therefore, the density of states at the Fermi level at low B ($\lesssim 1.5$ T in Fig. 3), where a great number of closely spaced energy levels (corresponding to several subbands) are occupied, will be a nearly smooth function of B , except when a subband is

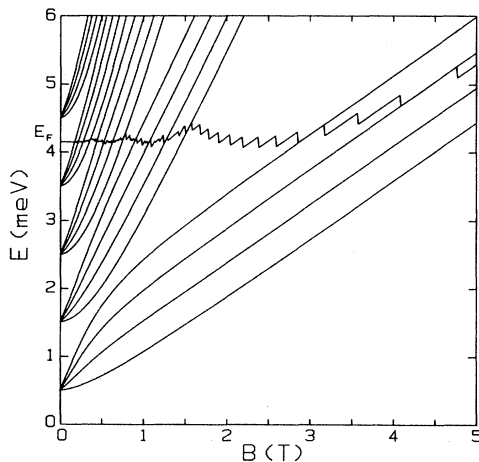


FIG. 3. Energy vs B fan diagram corresponding to $\theta = 10^\circ$ orientation is shown. For clarity, we show only every third level of the four lowest-lying eigenvalues of each subband. The position of E_F as a function of B is also shown. Spin splitting is not included.

depopulated, in which case it has a steplike discontinuity. For small θ , therefore, the low-field oscillations in ρ should occur as the subbands are depopulated, similar to the $\theta = 0^\circ$ case. At sufficiently high B ($\gtrsim 1.5$ T in Fig. 3), only energy levels corresponding to the lowest subband are occupied. New oscillations may then be expected provided that the width of the levels is small compared with the separation of the energy levels and that the temperature is sufficiently low. These oscillations should be periodic in $1/B$ since the degeneracy of each level is proportional to B .

Our experimental observations (Fig. 1) are in good agreement with the above predictions. First, we note that, as expected, the low-field oscillations corresponding to the depopulation of subbands for $\theta \lesssim 20^\circ$ are similar to those for $\theta = 0^\circ$.¹⁷ Second, assuming that the level degeneracy is equal to $(eB/h)\sin\theta$, we have indicated in Fig. 1 (vertical arrows) the field positions at which an integer number of (spin-split) levels are expected to be occupied. The minima observed in $\rho(B)$ data in Fig. 1 agree with the positions of these arrows in most cases.¹⁸ We note that for the self-consistent potential in the wide well described here, $V(z)$ is expected to be better approximated by a square well.^{3,4} In this case, the Hamiltonian of Eq. (2) can be solved in the high-field limit by using the adiabatic approximation,¹⁹ and gives the spectrum of the oblique states. These oblique states are localized in the x - y plane with the localization length in the \hat{x} direction, w_x , dependent on θ . Within the square-well approximation, w_x grows as $w/\tan\theta$ and the quantized energies scale as $E_n \tan^2\theta$, where E_n are the energies of the zero-field electric subband states in the square well. As $\theta \rightarrow 0^\circ$ and $B \rightarrow \infty$, w_x grows infinitely long and the oblique states go over into plane waves along the field in the lowest bulk Landau level (Fig. 2). Since the degeneracy of each state is given by $(eB/h)\sin\theta$, the oblique states should nevertheless produce Shubnikov-de Haas oscillations (periodic in $1/B$) as we have observed experimentally. However, since the energy levels of the oblique states for a square well are nonuniformly spaced in energy, accidental overlapping of the spin-split energy levels can occur. We expect minima at even filling factors for low fields where the spin-splitting is unresolved, and accidental degeneracies at higher fields where the spin splitting is large and the oblique levels are more closely spaced. The latter may account for the missing minima at particular filling factors in the data of Fig. 1. Further work aimed at a more quantitative understanding of the energy-level structure of a square well in a tilted magnetic field is planned.

Part of this work was performed at the Francis Bitter National Magnet Laboratory, which is supported at Massachusetts Institute of Technology by the National Science Foundation. We thank D. C. Tsui, K. Karrai, V. J. Goldman, and S. Das Sarma for useful discussions and L. Engel, B. Brandt, L. Rubin, and J. Moodera for technical assistance. Support of this work by the National Science Foundation Grants No. ECS-8553110, No. DMR-8705002, and No. DMR-8704670, and grants by the General Telephone and Electronics Laboratories, Inc., and the New Jersey Commission on Science and Technology is acknowledged.

- ¹T. Ando, A. B. Fowler, and F. Stern, *Rev. Mod. Phys.* **54**, 437 (1982).
- ²M. Shayegan, T. Sajoto, M. Santos, and C. Silvestre, *Appl. Phys. Lett.* **53**, 791 (1988).
- ³T. Sajoto, J. Jo, H. P. Wei, M. Santos, and M. Shayegan, *J. Vac. Sci. Technol. B* **7**, 311 (1989).
- ⁴T. Sajoto, J. Jo, L. Engel, M. Santos, and M. Shayegan, *Phys. Rev. B* **39**, 10464 (1989).
- ⁵K. Karrai, H. D. Drew, M. W. Lee, and M. Shayegan, *Phys. Rev. B* **39**, 1426 (1989).
- ⁶M. Sundaram, A. C. Gossard, J. H. English, and R. M. Westervelt, *Superlattices Microstruct.* **4**, 683 (1988).
- ⁷E. G. Gwinn, R. M. Westervelt, P. F. Hopkins, A. J. Rimberg, M. Sundaram, and A. C. Gossard, *Phys. Rev. B* **39**, 6260 (1989).
- ⁸To accurately determine the angle θ , we compared the Hall voltage at finite θ with its value at $\theta=90^\circ$. We estimate the accuracy in θ to be better than $\pm 0.2^\circ$. The position $\theta=0^\circ$ was achieved by minimizing the Hall voltage.
- ⁹J. Yoshino, H. Sakaki, and T. Hotta, *Surf. Sci.* **142**, 326 (1984).
- ¹⁰J. C. Maan, in *Two Dimensional Systems, Heterostructures, and Superlattices*, edited by G. Bauer, F. Kuchar, and H. Heinrich (Springer-Verlag, Berlin, 1984), p. 183.
- ¹¹In reality, as B increases, E_F oscillates near its value at $B=0$ as it crosses the energy levels, and monotonically decreases once it crosses the $N=1$ Landau level (the spin splitting is neglected here). Also, see Fig. 3.
- ¹²R. E. Doezema, M. Nealon, and S. Whitmore, *Phys. Rev. Lett.* **45**, 1593 (1980); M. Nealon, S. Whitmore, R. R. Bourassa, and R. E. Doezama, *Surf. Sci.* **113**, 282 (1982); J. C. Portal, R. J. Nicholas, M. A. Brummell, A. Y. Cho, K. Y. Cheng, and T. P. Pearsall, *Solid State Commun.* **43**, 907 (1982).
- ¹³A. Zrenner, H. Reisinger, F. Koch, K. Ploog, and J. C. Maan, *Phys. Rev. B* **33**, 5607 (1986).
- ¹⁴Th. Englert, J. C. Maan, D. C. Tsui, and A. C. Gossard, *Solid State Commun.* **45**, 989 (1983).
- ¹⁵Because of the spin splitting of the $n=0$ level at high B , another oscillation in ρ_l is expected around $B \approx 10$ T. We do indeed observe another structure in ρ_l around $B \approx 10$ T (not shown in Fig. 1).
- ¹⁶R. Merlin, *Solid State Commun.* **64**, 99 (1987).
- ¹⁷Comparison of our previously reported ρ_l data (Refs. 2 and 3) with data in Fig. 1 reveals that in our previous measurements (which were done in a cryostat without a tilting stage), θ deviated from 0° by a few degrees.
- ¹⁸We note that for $B > 5$ T, the measured Hall coefficient (at any θ) slightly deviated from its value at $B < 5$ T (e.g., at 7 T, the Hall coefficient was $\approx 8\%$ larger than its value at 5 T. This effect, which is likely to be a result of the magnetic-field-induced localization of carriers, may account for the discrepancy between the observed and expected positions of the minima in ρ above ~ 5 T.
- ¹⁹W. Trzeciakowski, M. Baj, S. Huant, and L. C. Brunel, *Phys. Rev. B* **33**, 6846 (1986).